Rapid and accurate structure determination of coiled-coil domains using NMR dipolar couplings: Application to cGMP-dependent protein kinase Iα

JASON R. SCHNELL,[1] GUO-PING ZHOU,[2] MARKUS ZWECKSTETTER,[3] ALAN C. RIGBY,[2] AND JAMES J. CHOU[1]

[1]Department of Biological Chemistry and Molecular Pharmacology and [2]Department of Medicine, Beth Israel Deaconess Medical Center, Harvard Medical School, Boston, Massachusetts 02115, USA
[3]Department of NMR-Based Structural Biology, Max Planck Institute for Biophysical Chemistry, 37077 Göttingen, Germany

(RECEIVED April 19, 2005; FINAL REVISION June 7, 2005; ACCEPTED June 21, 2005)

Abstract

Coiled-coil motifs play essential roles in protein assembly and molecular recognition, and are therefore the targets of many ongoing structural and functional studies. However, owing to the dynamic nature of many of the smaller coiled-coil domains, crystallization for X-ray studies is very challenging. Determination of elongated structures using standard NMR approaches is inefficient and usually yields low-resolution structures due to accumulation of small errors over long distances. Here we describe a solution NMR approach based on residual dipolar couplings (RDCs) for rapid and accurate structure determination of coiled-coil dimers. Using this approach, we were able to determine the high-resolution structure of the coiled-coil domain of cGMP-dependent protein kinase Iα, a protein of previously unknown structure that is critical for physiological relaxation of vascular smooth muscle. This approach can be extended to solve coiled-coil structures with higher order assemblies.

Keywords: coiled coil; residual dipolar coupling; NMR; cGMP-dependent protein kinase I

Coiled coils are protein interaction motifs that consist of left-handed supercoiled assemblies of two or more α helices. They are ubiquitous in nature, as they are found in > 5% of open reading frames (ORFs) in eukaryotic genomes (Newman et al. 2000). The length of coiled coils vary from protein to protein, with the longest being several hundred residues and the shortest being around 30 residues (Rose and Meier 2004). Very long coiled coils such as those found in intermediate filaments and myosin domains usually have structural and mechanical functions, whereas shorter coiled-coil domains often facilitate specific protein–protein oligomerizations in signaling and regulatory pathways (Lupas et al. 1991). The primary sequences of coiled coils consist of a characteristic repeating heptad of amino acids, denoted $(abcdefg)_n$, in which the *a* and *d* positions are predominantly hydrophobic, and the *e* and *g* positions are typically charged or polar. Assembly into oligomers results from hydrophobic residues packing together such that knobs pack into holes (Crick 1953; Harbury et al. 1993). Thus, some structural aspects of coiled coils are conserved and can be predicted from protein primary sequences (Lupas et al. 1991; Berger et al. 1995).

The molecular weight of typical coiled coils studied by solution NMR spectroscopy is small (< 15 kDa) because

Reprint requests to: James J. Chou, Department of Biological Chemistry and Molecular Pharmacology, Harvard Medical School, Boston, MA 02115, USA; e-mail: james_chou@hms.harvard.edu; fax: (617) 432-2921.

Article and publication are at http://www.proteinscience.org/cgi/doi/10.1110/ps.051528905.

the highly extended helical conformation results in a large rotational diffusion anisotropy (Tirado and de la Torre 1980). Since the amide N-H^N bond vectors all roughly point toward the long axis of the molecule, ^{15}N relaxation rates are unusually large and are in some cases comparable to globular proteins of ~45 kDa (Mackay et al. 1996). As a result of the extended helical conformation that is rich in methyl-bearing residues such as leucine, valine, and isoleucine, the methyl resonances are typically poorly resolved. Moreover, since NOEs are qualitative distance restraints, the subtle deviation from the backbone of ideal straight helices can only be detected by a large number of local and intermolecular NOEs quantified with different NOESY mixing times. At the same time, without long-range information, small local inaccuracies in the structure determination can be propagated into large deviations over the length of the coiled coil.

Residual dipolar couplings (RDCs) are exquisitely sensitive to bond vector orientation (Tolman et al. 1995; Tjandra and Bax 1997), and are therefore uniquely suited for characterizing the bending of α-helices (Chou et al. 2002) that occurs in coiled-coil structures. It is not possible to pack the constituent monomers into a dimer using only RDCs, since dipolar couplings do not provide translational information. However, assembly can be accomplished using the conserved properties of coiled-coil packing because without exceptions, the *a* and *d* positions of the heptad repeat make up the core of the helix–helix interface, and the *e* and *g* positions occupy the region between the core and the solvent. This permits the development of an RDC-based approach for rapid and accurate structure determination of coiled-coil dimers that does not involve the time-consuming process of assigning NOE-derived distance restraints. It involves (1) measuring RDCs for proteins marginally aligned in the filamentous phage (Pf1) liquid crystalline medium, (2) identifying the coiled-coil motif by RDC-based molecular replacement analysis, (3) defining the subtle curvature and supercoiling of the constituent helices by RDC refinement, (4) assembling parallel and anti-parallel models of the coiled-coil dimer using knowledge-based intermolecular distance restraints, and (5) deriving the correct monomer–monomer orientation by comparing experimental RDCs with those predicted from the three-dimensional charge distribution and shape of the alternative structural models.

The approach is demonstrated here for the coiled-coil domain of the cGMP-dependent protein kinase I (cGK1α), which functions in the nitric oxide (NO)-mediated relaxation of vascular smooth muscle (Lincoln 1994). The state of contraction or relaxation of vascular smooth muscle cells is closely coupled to phosphorylation and dephosphorylation of the regulatory myosin light chain, which is in part regulated by the binding of cGK1α to the myosin-binding subunit (MBS) of the myosin phosphatase (Surks et al. 1999). It has been recently demonstrated that this binding is mediated by the interaction between a coiled-coil-containing region (residues 1–59) of cGK1α and the leucine/isoleucine zipper of MBS (Surks and Mendelsohn 2003). A number of mutagenesis studies have suggested that $cGK1\alpha^{1-59}$ forms a coiled-coil dimer of which the zipper region may be responsible for interaction with MBS (Atkinson et al. 1991; Surks and Mendelsohn 2003). Hence, the high-resolution structure of the cGK1α coiled-coil dimer, which is not yet known, is the first step toward the understanding of cGK1α-MBS recognition.

Results and Discussion

Identification of the coiled-coil segment in $cGK1\alpha^{1-59}$

Sequence-based prediction of the coiled-coil region of $cGK1\alpha^{1-59}$ was made using the programs COILS (Lupas et al. 1991) and PAIRCOIL (Berger et al. 1995). Both programs identified the region to be approximately 38 amino acids in length, commencing at residue 9 and continuing through residue 46 (Fig. 1A). The structured helical region of $cGK1\alpha^{1-59}$ was independently examined by ^{15}N R_1 and R_2 relaxation rates (Fig. 1B), which indicated that for residues 9–44, the T_1/T_2 ratio is quite uniform but decreases sharply as the sequence is extended beyond 9–44 at both N- and C-terminal ends. The results from sequence prediction and relaxation measurements indicate that it is valid to treat the backbone of residues 9–44 as a rigid molecule for dipolar coupling refinement.

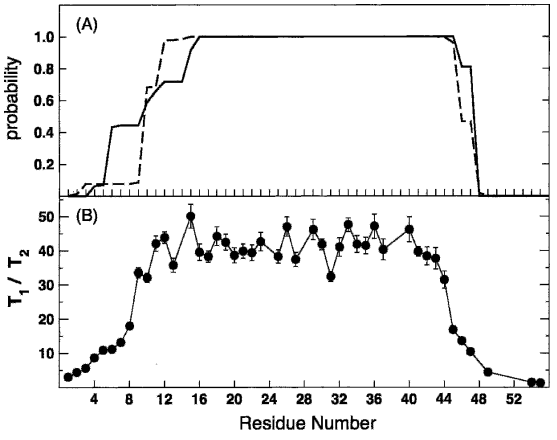

Figure 1. Determination of the coiled-coil region of $cGK1\alpha^{1-59}$ by sequence-based coiled-coil prediction using the programs COILS and PAIRCOILS (*A*) and ratio of the backbone amide ^{15}N longitudinal (T_1) and transverse (T_2) relaxation times (*B*). ^{15}N relaxation data were recorded at a ^1H spectrometer frequency of 500 MHz. The pulse sequence used closely followed that of Farrow et al. (1994) with sensitivity enhancement and coherence selection via pulsed-field gradients.

To characterize the coiled-coil region by RDCs, a sample of cGK1α$^{1–59}$ was weakly aligned under a strong magnetic field by adding 15 mg/mL of the filamentous phage Pf1. The observed amide chemical shift resonances of cGK1α$^{1–59}$ in Pf1 liquid crystal were essentially identical to that of the isotropic sample without Pf1, indicating that perturbation of the protein by the alignment medium is minimal. Three types of backbone dipolar couplings—$^{1}D_{NH}$, $^{1}D_{C'C\alpha}$, and $^{1}D_{C'N}$—were measurement for structural analysis.

A preliminary model of the monomeric helix in the cGK1α coiled coil was found by fitting experimental RDCs to segments of coiled-coil α-helices in the database, analogous to the molecular fragment replacement method described previously (Delaglio et al. 2000). Here we used the 2.7 Å crystal structure of the 14-heptad repeat coiled-coil domain of cortexillin I from *Dictyostelium discoideum* (Burkhard et al. 2000). This parallel coiled-coil dimer is 101 residues long and contains a full superhelical turn. The backbone RDCs of residues 9–44 were systematically fit to all 36-residue segments of the crystal structure in a sliding window manner. While the segments are qualitatively similar, their agreements with experimental RDCs varied significantly with the Pearson correlation coefficient (r) ranging from 0.84 to 0.95 and the quality factor (Q), from 0.31 to 0.53 (Fig. 2A), further emphasizing the strength of dipolar couplings in describing the less obvious features of α-helices.

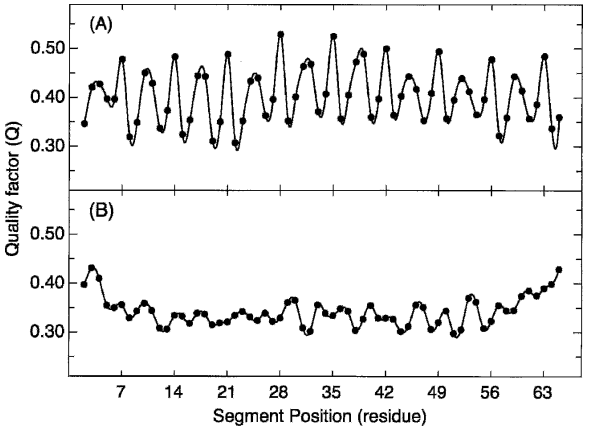

Figure 2. Singular-value-decomposition (SVD) method evaluation of the goodness of fit for the measured RDCs to structural models. The SVD correlation was calculated in a sliding-window manner using the program PALES (Zweckstetter and Bax 2000) to the 101-residue cortexillin parallel coiled-coil dimer (*A*) (1D7M; Burkhard et al. 2000) and 101 residues of an approximately straight helix generated in an XPLOR refinement (*B*) in which canonical φ,ψ angles and intrahelical hydrogen bonds were strictly enforced. The goodness of fit was assessed by the quality factor (Q) (Cornilescu et al. 1998). Points were interpolated using a cubic spline in order to highlight periodicity in the goodness of fit.

Remarkably, when sliding position *a* of the first heptad of cGK1α$^{1–59}$ against the crystal structure, both r and Q showed a pronounced wave-like pattern having the exact heptad periodicity that is characteristic of coiled coils. This is because in a supercoiled helix, the helical turns at the packing interface (residues *a*, *d*, *e*, and *g*) are slightly compressed while those facing outside (residues *b*, *c*, and *f*) are stretched, analogous to the bending of a spring. This leads to periodic disagreement when RDCs are fit to a segment of coiled coil that is out of register. Q is maximum when RDCs for the coiled-coil interior positions *a* and *d* are in register with the exterior positions *f* and *b*, respectively, of the structural model. Alternatively, Q is minimum when the heptad repeat is in register, or nearly so. Surprisingly, the quality of fit when RDCs for positions *a* and *d* of cGK1α$^{9–44}$ corresponded to positions *g* and *c* of the structural model was as good as or better than when the heptads were fully in register. The source of this degeneracy is unknown, but may be attributable to the specific details of how cGK1α$^{9–44}$ assembles, the resolution of the structural model, or the accuracy of the RDC measurements. When performing similar fittings to a regular α-helix, no patterns could be recognized (Fig. 2B). The wave-like patterns of dipolar couplings have been used to characterize helical structures (Mesleh et al. 2002). Here we show that the correlation between dipolar couplings and known coiled-coil structures also acquires a wave-like pattern when there is systematic bending of a helix, and the heptad periodicity can be used to directly conclude whether or not the protein under study is a coiled-coil even in the absence of sequence-based coiled-coil predictions.

Refinement of the constituent helix

The backbone segment of cortexillin with the best overall fit against RDCs (residues 257–292) (Fig. 2A) was subjected to dipolar coupling refinement to yield the monomer structure. Refinement was performed using the program XPLOR-NIH (Schwieters 2002) according to the low-temperature simulated annealing (SA) protocol described previously (Chou et al. 2000b, 2001) (see Materials and Methods for details). Values of the magnitude (D_a) and rhombicity (R) of the alignment tensor required by the XPLOR protocol were determined from the extended histogram method (EHM) (Bryce and Bax 2004) to be −19.9 Hz (normalized to $^{1}D_{NH}$) and 0.13, respectively. An ensemble of 20 structures were calculated with experimental RDCs, consisting of three backbone couplings per residue, as well as side chain χ^1 angles derived from $^{3}J_{NC\gamma}$ and $^{3}J_{C'C\gamma}$ scalar couplings. To examine whether RDC refinement was meaningful, a series of cross-validations were performed. This was achieved by randomly excluding 15% (16 out of 108)

of the backbone couplings that are uniformly distributed along the peptide during refinement and using them to validate the refined structure by an SVD fit. The process was repeated 100 times to allow for meaningful statistics. Before refinement, the average Q was 0.21 with standard deviation of 0.06. After refinement, the average Q is improved to 0.15 with standard deviation of 0.06.

Building alternative dimer models

Having an accurate structure of the constituent helices, which exhibits a subtle bending expected for a coiled-coil structure, a preliminary model of the dimer was built by satisfying the characteristic side-chain packing of the residues in the heptad repeats. A representative set of leucine–leucine parallel coiled-coil interactions, which had been obtained at high-resolution using X-ray crystallography, were extracted from the Protein Data Bank (PDB) in order to implement knowledge-based restraints on the intermolecular packing. Table 1 presents the intermolecular distances between the γ-carbons of leucines and isoleucines at the *a* and *d* positions for parallel and anti-parallel dimers. To investigate whether it is possible to use RDCs to distinguish parallel packing from anti-parallel packing in the absence of biochemical data, both parallel and anti-parallel dimers were assembled. The models can be built either manually or using a structure calculation protocol. Here the dimers were built in XPLOR by using the rigid-body dynamics option (Schwieters et al. 2002). In this case, the backbones of individual monomers were treated as rigid body while the side chains were allowed to move. The calculations were done in the presence of experimental χ^1 restraints and knowledge-based intermolecular distance restraints. For the parallel dimer, the distance between intermolecular Cγ atoms for leucines in heptad position *a* (L12, L26, and L40) and position *d* (L22 and L36) were set according to the values listed in Table 1. For the anti-parallel dimer, the distance between intermolecular leucine Cγ and isoleucine $C\gamma_1/\gamma_2$ atoms were set to 5.0 Å. At the end of calculations, no distances larger than 0.25 Å were violated and in both cases the supercoiling is left-handed, consistent with all known heptad-based coiled-coil structures. Therefore, without additional considerations, RDC refinement alone cannot be used to distinguish between parallel and anti-parallel packing.

Table 1. *Intermolecular distances in coiled-coil dimer*[a]

Orientation	Heptad position	Occurrences	Distance (Å)
Parallel	*a*	19	5.5 (0.9)
Parallel	*d*	39	5.4 (0.4)
Anti-parallel[b]	*a*/*d*	14	5.0 (0.6)

[a] Distances are Cγ to Cγ for coiled-coil dimers taken from the PDB. The leucine pairs measured were restricted to those that had a predicted coiled-coil probability of greater than 0.7 (Berger et al. 1995). The numbers in parentheses are the standard deviations. The PDB accession numbers of the structures of parallel coiled-coil dimers are cortexillin, 1D7M; APC protein, 1DEB; vimentin, 1GK6; MAD-1, 1GO4; chicken tropomyosin α chain, 1IC2; EEA1, 1JOC; scallop myosin, 1NKN; yeast GCN4, 2ZTA. The PDB accession numbers of the anti-parallel coiled-coil homodimers are hepatitis δ antigen, 1A92; F1 ATPase inhibitor, 1GMJ; copper efflux regulator, 1Q05; proline porter II, 1R48.
[b] In the anti-parallel case, *a*/*d* pairs with leucine to isoleucine and vice versa were measured. For isoleucine, the position of Cγ was taken as halfway between Cγ1 and Cγ2.

The parallel and anti-parallel dimer models were then subject to a second round of global refinement (without the rigid-body implementation) to ensure that experimentally derived restraints of the constituent monomers could be simultaneously satisfied in the dimer structure. In this step, which uses the same XPLOR protocol (see Materials and Methods for details), identical intramolecular restraints—including RDCs, backbone φ and ψ derived from the model, and side-chain χ^1 angles derived from three-bond *J* couplings—are assigned to both monomers. To keep the dimer intact, the same knowledge-based distance restraints used above were enforced. The 20 parallel structures, which were subsequently proven to have the correct packing mode (see below), are shown in Figure 3A. The refinement statistics are given in Table 2.

Parallel vs. anti-parallel dimer

In order to derive the correct monomer–monomer orientation, experimental RDCs were compared with values predicted from the three-dimensional structural models of the parallel and anti-parallel dimer. Since the Pf1 surface is negatively charged, an interaction with Pf1 that results in the weak alignment of the protein is composed of both steric and electrostatic components (Zweckstetter et al. 2004). It has been previously demonstrated that by using a simplified computational model, protein RDCs in liquid crystalline media, such as Pf1, could be predicted with reasonable accuracy from the three-dimensional charge distribution and shape of the protein (Zweckstetter and Bax 2000). Although the overall shapes of the parallel and anti-parallel dimer are similar and almost indistinguishable by steric alignment prediction, their charge distributions are very different, enabling the addition of charge-predicted alignment to find the unique solution of the packing mode. For alignment tensor prediction using the program PALES (Zweckstetter and Bax 2000), the atomic coordinates of the well-structured region, residues 9–44 of cGK1α, were used. To account for structural uncertainty and dynamics, the alignment tensor was averaged over an ensemble of 20 structures with lowest dipolar energy calculated for parallel and anti-parallel dimers. When using only the shape-based prediction component

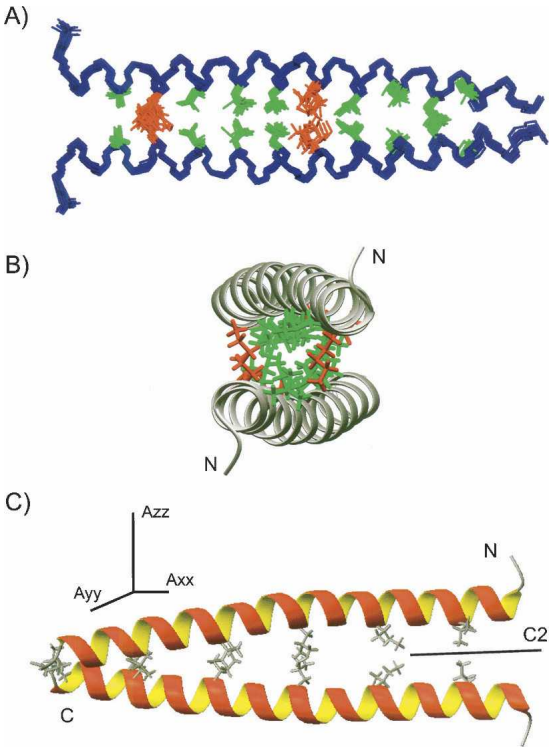

Figure 3. Structure of the coiled-coil domain of cGK1α. (*A*) Bundle of 20 refined parallel coiled-coil dimer structures with lowest RDC energies superimposed on the backbone heavy atoms (blue). The hydrophobic side chains of leucine and isoleucine in positions *a* and *d* are shown in green, and the two side chains of lysine, which are in position *d*, are shown in red. (*B*) End-on view from the N terminus of a representative refined dimer. The backbone structure is shown as a ribbon diagram, and side chains are colored as in *A*. (*C*) Ribbon representation of the coiled-coil dimer oriented relative to the principal axis frame of the alignment tensor (A_{XX}, A_{YY}, A_{ZZ}), showing the small angle (4°) between A_{XX} and the axis of molecular symmetry. Structure representations were generated using MOLMOL (Koradi et al. 1996).

of the program, we found that the alignment tensors were both axially symmetric, with magnitude of -11.4 ± 0.2 Hz and -11.3 ± 0.2 Hz for the parallel and the anti-parallel structures, respectively. However, by activating both steric and electrostatic prediction components in PALES (Zweckstetter et al. 2004), the experimental RDCs agreed very well with RDCs predicted from the parallel dimers (average correlation coefficient $r = 0.94$) but very poorly with those derived from the anti-parallel structures ($r = 0.39$); this indicated that the parallel dimer is the correct structure. The structure of the parallel dimer is shown in Figure 3, B and C.

The C2 symmetry

In an ideal case of rigid molecule, A_{XX} is parallel to the C2 axis (Tjandra et al. 1996; Prestegard et al. 2000). To examine the degree of correlation between molecular symmetry and the principal axes of the alignment tensor, the 20 structures were fitted to all RDCs of residues 9–44 to determine the Euler angles. Upon rotating the PDB coordinates to the principal axis frame, the molecular symmetry axis is almost, but not exactly, parallel to the A_{XX} of the tensor, with an average angle of $2.7 \pm 1.8°$ between the two axes (Fig. 3C). The small deviation from the ideal scenario could be attributed to errors in the structure and/or RDC measurement.

Conclusions

We have demonstrated that NMR dipolar couplings can be used to identify the coiled-coil heptad repeats, and by

Table 2. *Structural statistics and atomic RMS differences*[a]

Structural statistics		
RMSD from experimental		
Dipolar coupling restraints (Hz)[b,c]		
Backbone (108/108)		2.15
NH	(35/35)	1.52
$C'C^{\alpha}$	(36/36)	2.52
NC'	(37/37)	2.28
Other restraints[c,d]		
H-bond (Å)	(38/38)	0.026
ϕ/ψ (deg)	(43/43)	0
χ^1 (deg)	(18/18)	0
Deviations from idealized covalent geometry		
Bonds (Å)		0.0026
Angles (deg)		0.33
Impropers (deg)		0.30
Energy (kcal mol^{-1})		
Dipolar		141
Dihedral		1.5
H-bond		3.2
Repel		28.1
ϕ/ψ in most favored region (%)[e]		96.4
Q_{free} (%)[f]		16
Atomic RMS differences (Å)[a]		
Backbone		0.50
All heavy atoms		1.16

[a] Statistics are calculated and averaged over 20 simulated annealing structures obtained from the protocol described in the text. The precision of the atomic coordinates is defined as the average RMS differences between the 20 final structures and their mean coordinates.
[b] The RMS difference between individual sets of experimental dipolar couplings and those predicted by refined structures (averaged over 20 structures) by means of SVD fit. All couplings are normalized to $^1D_{NH}$.
[c] Number of restraints is listed per monomer.
[d] None of the structures has H-bond restraint violation >0.25 Å, ϕ/ψ and χ^1 restraints violation $>5°$.
[e] As evaluated with the program PROCHECK (Laskowski et al. 1993).
[f] Q_{free} is the free quality factor (Cornilescu et al. 1998), which was obtained by randomly excluding 15% (32 out of 216 in the dimer) of the backbone couplings that are uniformly distributed along the peptide during refinement and using them to validate the refined structure by a SVD fit. The process was repeated 100 times, and the average quality factor is presented.

employing knowledge-based constraints, determine the high-resolution structure. Since measurement of RDCs requires only sequence-specific assignment of protein backbone chemical shifts, which is relatively straightforward using standard triple-resonance experiments (Kay et al. 1990), this approach for rapid structure determination can be easily automated. The structure of the coiled-coil region of cGK1α determined here is new, and will contribute to the understanding of molecular recognition between cGK1α and MBS. Although the approach is demonstrated for a coiled-coil dimer, it is expected to be applicable for higher order assemblies such as coiled-coil trimers and tetramers. Since the ^{15}N R_2 relaxation rate is largely governed by the α-helical length, it will not significantly increase upon the addition of helices into higher order oligomers. The ability to quickly and accurately determine the structure of coiled coils will facilitate our understanding of the multitude of protein–protein interactions mediated by this motif.

Materials and methods

Sample preparation

Human wild-type cGK1α$^{1-59}$ gene encompassing the coiled-coil region was cloned into the pGEX-2T vector and expressed in *Escherichia coli* with GST fused at the N terminus. The amino acid sequence after thrombin cleavage was *GSPGIPGST*-T^{1}SELEEDFAK^{10}ILMLKEERIK^{20}ELEKRLSEKE^{30}EEIQEL KRKL^{40}HKCQSVLPVP^{50}STHIGPRTT. The natural sequence of cGK1α starts from Thr 1. The transformed cells were grown in either LB-rich media (for unlabeled protein) or M9-minimal media (for isotope-labeled protein). For isotope labeling, the M9 media were substituted with ^{15}N-labeled ammonium chloride. For triple-resonance experiments, uniformly ^{15}N-, ^{13}C-, ^{2}H-labeled protein was prepared by growing the cells in 90% D_2O with ^{15}N-ammonium chloride and ^{13}C-glucose. A total of two NMR samples were used for the present study, each prepared in 260 μL of 95% H_2O/5% D_2O (pH 7.0), using 280-μL Shigemi microcells. The isotropic sample contained 1 mM protein, 20 mM potassium phosphate, 10 mM NaCl, 1 mM EDTA, 5 mM DTT, and 1 mM azide. The aligned sample used for structure determination contained 15 mg/mL of the filamentous phage Pf1 (Asla Labs), 1 mM protein, 20 mM potassium phosphate, 10 mM NaCl, 1 mM EDTA, 5 mM DTT, and 1 mM Azide.

NMR measurement

All NMR experiments were conducted on Bruker spectrometers equipped with cryogenic probes at 30°C. Sequence-specific backbone assignments of residues 1–55 were accomplished using a standard suite of triple-resonance experiments including the TROSY versions of HNCA, HNCACB, HNCACO, and HNCO (Kay et al. 1990; Salzmann et al. 1999).

Three types of backbone dipolar couplings were measured: $^{1}D_{NH}$, $^{1}D_{C'C\alpha}$, and $^{1}D_{C'N}$. The ^{1}H-^{15}N couplings were measured at 600 MHz (^{1}H frequency) by interleaving the 3D HNCO experiments (Ikura et al. 1990), with and without ^{1}H CPD decoupling (Kontaxis et al. 2000), both acquired with 50 msec of mixed-CT ^{15}N evolution. The $^{13}C'$-$^{13}C^{\alpha}$ couplings were obtained at 500 MHz from the standard 3D HNCO recorded with 100 msec of $^{13}C^{\alpha}$-coupled $^{13}C'$ evolution. The one-bond $^{13}C'$-N couplings were measured at 600 MHz using the 3D TROSY-HNCO in a quantitative-J manner (Chou et al. 2000a). On the basis of the length of the time domain data and the signal to noise (Kontaxis et al. 2000), the estimated average errors for $^{1}D_{NH}$ and $^{1}D_{C'C\alpha}$ are ±0.2 Hz and ±0.1 Hz, respectively. For $^{1}D_{NC'}$ derived from the quantitative J experiment, the average error is estimated to be ±0.2 Hz based on the error analysis previously described (Chou et al. 2000a).

Measurements of $^{3}J_{C'C\gamma}$ and $^{3}J_{NC\gamma}$ coupling constants for determining side-chain χ_1 rotamers were carried out at 500 MHz for couplings involving $^{13}C'$ and at 600 MHz for couplings involving ^{15}N, using standard two-dimensional quantitative J methods (Hu and Bax 1997; Hu et al. 1997a,b). Longitudinal (T_1) and transverse (T_2) ^{15}N relaxation data were recorded at a ^{1}H spectrometer frequency of 500 MHz. The pulse sequences used closely followed that of Farrow et al. (1994) with sensitivity enhancement and coherence selection via pulsed-field gradients.

Data processing and spectra analyses were done in NMRPipe (Delaglio et al. 1995). RDCs were extracted by subtracting isotropic couplings from the aligned couplings. Fitting of the dipolar couplings to structures was done by singular value decomposition (Losonczi et al. 1999), using the program PALES (Zweckstetter and Bax 2000). The goodness of fit was assessed by both Pearson correlation coefficient (r) and the quality factor (Q) (Cornilescu et al. 1998).

Structure calculation protocol

Dipolar coupling refinement of structural models were performed using the program XPLOR-NIH (Schwieters et al. 2002) according to the low-temperature simulated annealing (SA) protocol described previously (Chou et al. 2000b, 2001). Structural restraints were applied only for residues 9–44, the rigid α-helical region as indicated by ^{15}N relaxation data, Cα/Cβ chemical shifts and RDC values.

In the case of monomer refinement, the starting model was a segment from the crystal structure of cortexillin that best matches the experimental RDCs. Refinement used the three sets of measured RDCs ($^{1}D_{NH}$, $^{1}D_{C'C\alpha}$, and $^{1}D_{C'N}$) and side-chain χ^1 angles derived from $^{3}J_{NC\gamma}$ and $^{3}J_{C'C\gamma}$ scalar couplings. Backbone torsion angle restraints were derived from the starting model, all having a flat-well (±10°) harmonic potential with force constant fixed at 200 kcal mol^{-1} rad^{-2}. Hydrogen bond distance restraints of 2 Å and 3 Å (O—H^N and O—N, respectively) were enforced for the rigid helical region, with flat-well (±0.2 Å) harmonic potentials, and a force constant fixed at 20 kcal mol^{-1} Å^{-2}. For dimer refinement in which knowledge-based intermolecular distance restraints for leucine residues in the *a* or *d* heptad position are used, these artificial NOE restraints are also enforced by flat-well (±0.2 Å) harmonic potentials, with the force constant fixed at 30 kcal mol^{-1} Å^{-2}. For side chains that are more or less "locked" into nearly ideal χ^1 staggered rotamers on the basis of comparing of $^{3}J_{C'C\gamma}$ and $^{3}J_{NC\gamma}$ couplings, flat-well (±30°) harmonic χ^1 potentials are applied with force constant fixed at 20 kcal mol^{-1} rad^{-2}. In addition to the experimental χ^1 restraints, a weak database-

derived "Rama" potential function in XPLOR (Kuszewski et al. 1997) is ramped from 0.02 to 0.2 (dimensionless force constant) for the general treatment of side-chain rotamers. Finally, RDC restraint force constant is ramped from 0.0002 to 0.1 kcal mol^{-1} Hz^{-2} (normalized for the $^1D_{NH}$ couplings). Other force constants, commonly used in NMR structure calculation, are $k(\text{vdw}) = 0.002 \rightarrow 4.0$ kcal mol^{-1} $Å^{-2}$; $k(\text{impr}) = 0.1 \rightarrow 1.0$ kcal mol^{-1} $degree^{-2}$; and k(bond angle) $= 0.4 \rightarrow 1.0$ kcal mol^{-1} $degree^{-2}$. During the annealing run, the bath is cooled from 300 to 20 K with a temperature step of 10 K, and 6.7 psec of Verlet dynamics at each temperature step, using a time step of 3 fsec.

The coordinates of cGK1α^{9-44} have been deposited to the PDB with ID 1ZXA.

Acknowledgments

We thank Dr. M.E. Mendelsohn and Dr. H.K. Surks for the cGK1α construct and helpful discussions throughout. This study was supported by an Atorvastatin Research Award from Pfizer to A.C.R., a DFG Emmy Noether-Grant (ZW 71/1-4) to M.Z., and the Smith Family Award for Young Investigators and the PEW Scholarship to J.J.C.

References

Atkinson, R., Saudek, V., Huggins, J., and Pelton, J. 1991. ^{1}H NMR and circular dichroism studies of the N-terminal domain of cyclic GMP dependent protein kinase: A leucine/isoleucine zipper. *Biochemistry* **30:** 9387–9395.

Berger, B., Wilson, D., Wolf, E., Tonchev, T., Milla, M., and Kim, P. 1995. Predicting coiled coils by use of pairwise residue correlations. *Proc. Natl. Acad. Sci.* **92:** 8259–8263.

Bryce, D.L. and Bax, A. 2004. Application of correlated residual dipolar couplings to the determination of the molecular alignment tensor magnitude of oriented proteins and nucleic acids. *J. Biomol. NMR* **28:** 273–278.

Burkhard, P., Kammerer, R.A., Steinmetz, M.O., Bourenkov, G.P., and Aebi, U. 2000. Coiled-coil dimerization domain from cortexillin I. *Structure* **8:** 223–230.

Chou, J.J., Delaglio, F., and Bax, A. 2000a. Measurement of one-bond ^{15}N-^{13}C′ dipolar couplings in medium sized proteins. *J. Biomol. NMR* **18:** 101–105.

Chou, J.J., Li, S.P., and Bax, A. 2000b. Study of conformational rearrangement and refinement of structural homology models by the use of heteronuclear dipolar couplings. *J. Biomol. NMR* **18:** 217–227.

Chou, J.J., Li, S.P., Klee, C.B., and Bax, A. 2001. Solution structure of Ca^{2+}-calmodulin reveals flexible hand-like properties of its domains. *Nat. Struct. Biol.* **8:** 990–997.

Chou, J.J., Kaufman, J.D., Stahl, S.J., Wingfield, P.T., and Bax, A. 2002. Micelle-induced curvature in a water-insoluble HIV-1 Env peptide revealed by NMR dipolar coupling measurement in stretched polyacrylamide gel. *J. Am. Chem. Soc.* **124:** 2450–2451.

Cornilescu, G., Marquardt, J.L., Ottiger, M., and Bax, A. 1998. Validation of protein structure from anisotropic carbonyl chemical shifts in a dilute liquid crystalline phase. *J. Am. Chem. Soc.* **120:** 6836–6837.

Crick, F.H.C. 1953. The packing of α-helices: Simple coiled-coils. *Acta Crystallogr.* **6:** 689–697.

Delaglio, F., Grzesiek, S., Vuister, G.W., Zhu, G., Pfeifer, J., and Bax, A. 1995. NMRPipe: A multidimensional spectral processing system based on UNIX pipes. *J. Biomol. NMR* **6:** 277–293.

Delaglio, F., Kontaxis, G., and Bax, A. 2000. Protein structure determination using molecular fragment replacement and NMR dipolar couplings. *J. Am. Chem. Soc.* **122:** 2142–2143.

Farrow, N.A., Muhandiram, R., Singer, A.U., Pascal, S.M., Kay, C.M., Gish, G., Shoelson, S.E., Pawson, T., Forman-Kay, J.D., and Kay, L.E. 1994. Backbone dynamics of a free and a phosphopeptide-complexed Src homology 2 domain studied by ^{15}N NMR relaxation. *Biochemistry* **33:** 5984–6003.

Harbury, P.B., Zhang, T., Kim, P.S., and Alber, T. 1993. A switch between two, three, and four-stranded coiled coils in GCN4 leucine zipper mutants. *Science* **262:** 1401–1407.

Hu, J.-S. and Bax, A. 1997. Determination of φ and χ1 angles in proteins from ^{13}C-^{13}C three-bond J couplings measured by three-dimensional heteronuclear NMR. How planar is the peptide bond? *J. Am. Chem. Soc.* **119:** 6360–6368.

Hu, J.-S., Grzesiek, S., and Bax, A. 1997a. χ1 angle information from a simple two-dimensional NMR experiment which identifies trans 3JNCg couplings in isotopically enriched proteins. *J. Biomol. NMR* **9:** 323–328.

———. 1997b. Two-dimensional NMR methods for determining c1 angles of aromatic residues in proteins from three-bond JC′Cg and JNCg couplings. *J. Am. Chem. Soc.* **119:** 1803–1804.

Ikura, M., Kay, L.E., and Bax, A. 1990. A novel approach for sequential assignment of ^{1}H, ^{13}C, and ^{15}N spectra of larger proteins: Heteronuclear triple-resonance three-dimensional NMR spectroscopy application to calmodulin. *Biochemistry* **29:** 4659–4667.

Kay, L.E., Ikura, M., Tschudin, R., and Bax, A. 1990. Three-dimensional triple resonance NMR spectroscopy of isotopically enriched proteins. *J. Magn. Reson.* **89:** 496–514.

Kontaxis, G., Clore, G., and Bax, A. 2000. Evaluation of cross-correlation effects and measurement of one-bond couplings in proteins with short transverse relaxation times. *J. Magn. Reson.* **143:** 184–196.

Koradi, R., Billeter, M., and Wuthrich, K. 1996. MOLMOL: A program for display and analysis of macromolecular structures. *J. Mol. Graph.* **14:** 51–55.

Kuszewski, J., Gronenborn, A.M., and Clore, G.M. 1997. Improvements and extensions in the conformational database potential for the refinement of NMR and X-ray structures of proteins and nucleic acids. *J. Magn. Reson.* **125:** 171–177.

Laskowski, R.A., MacArthur, M.W., Moss, D.S., and Thornton, J.W. 1993. PROCHECK: A program to check the stereochemical quality of protein structures. *J. Appl. Crystallogr.* **26:** 283–291.

Lincoln, T.M. 1994. *Cyclic GMP: Biochemistry, physiology and pathophysiology*, 1st ed, pp. 98–100. R.G. Landes Co., Austin, TX.

Losonczi, J.A., Andrec, M., Fischer, M.W.F., and Prestegard, J.H. 1999. Order matrix analysis of residual dipolar couplings using singular value decomposition. *J. Magn. Reson.* **138:** 334–342.

Lupas, A., Van Dyke, M., and Stock, J. 1991. Predicting coiled coils from protein sequences. *Science* **24:** 1162–1164.

Mackay, J.P., Shaw, G.L., and King, G.F. 1996. Backbone dynamics of the c-jun leucine zipper: ^{15}N NMR relaxation studies. *Biochemistry* **35:** 4867–4877.

Mesleh, M.F., Veglia, G., DeSilva, T.M., Marassi, F.M., and Opella, S.J. 2002. Dipolar waves as NMR maps of protein structure. *J. Am. Chem. Soc.* **124:** 4206–4207.

Newman, J.R., Wolf, E., and Kim, P.S. 2000. A computationally directed screen identifying interacting coiled coils from *Saccharomyces cerevisiae*. *Proc. Natl. Acad. Sci.* **97:** 13203–13208.

Prestegard, J.H., al-Hashimi, H.M., and Tolman, J.R. 2000. NMR structures of biomolecules using field oriented media and residual dipolar couplings. *Q. Rev. Biophys.* **33:** 371–424.

Rose, A. and Meier, I. 2004. Scaffolds, levers, rods and springs: Diverse cellular functions of long coiled-coil proteins. *Cell Mol. Life Sci.* **61:** 1996–2009.

Salzmann, M., Wider, G., Pervushin, K., and Wuthrich, K. 1999. Improved sensitivity and coherence selection for [15N,1H]-TROSY elements in triple resonance experiments. *J. Biomol. NMR* **15:** 181–184.

Schwieters, C.D., Kuszewski, J., Tjandra, N., and Clore, G.M. 2002. The Xplor-NIH NMR molecular structure determination package. *J. Magn. Reson.* **160:** 66–74.

Surks, H.K. and Mendelsohn, M.E. 2003. Dimerization of cGMP-dependent protein kinase 1α and the myosin-binding subunit of myosin phosphatase: Role of leucine zipper domains. *Cell. Signal.* **15:** 937–944.

Surks, H.K., Mochizuki, N., Kasai, Y., Georgescu, S.P., Tang, K.M., Ito, M., Lincoln, T.M., and Mendelsohn, M.E. 1999. Regulation of myosin phosphatase by a specific interaction with cGMP-dependent protein kinase Iα. *Science* **286:** 1583–1587.

Tirado, M.M. and de la Torre, J.G. 1980. Rotational dynamics of rigid, symmetric top macromolecules. Application to circular cylinders. *J. Chem. Phys.* **73:** 1986–1993.

Tjandra, N. and Bax, A. 1997. Direct measurement of distances and angles in biomolecules by NMR in a dilute liquid crystalline medium. *Science* **278:** 1111–1114.

Tjandra, N., Wingfield, P., Stahl, S., and Bax, A. 1996. Anisotropic rotational diffusion of perdeuterated HIV protease from ^{15}N NMR relaxation measurements at two magnetic fields. *J. Biomol. NMR* **8:** 273–284.

Tolman, J., Flanagan, J., Kennedy, M., and Prestegard, J. 1995. Nuclear magnetic dipole interactions in field-oriented proteins—Information for structure determination in solution. *Proc. Natl. Acad. Sci.* **92:** 9279–9283.

Zweckstetter, M. and Bax, A. 2000. Prediction of sterically induced alignment in a dilute liquid crystalline phase: Aid to protein structure determination by NMR. *J. Am. Chem. Soc.* **122:** 3791–3792.

Zweckstetter, M., Hummer, G., and Bax, A. 2004. Prediction of charge-induced molecular alignment of biomolecules dissolved in dilute liquid-crystalline phases. *Biophys. J.* **86:** 3444–3460.